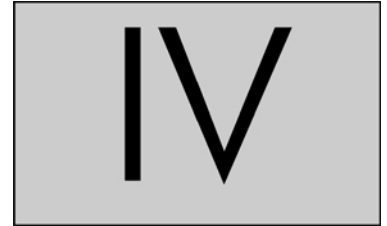
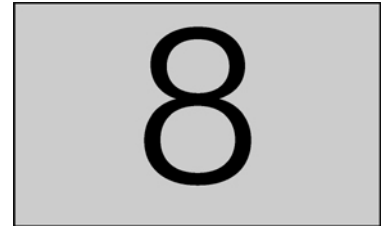


Dynamics



Unentangled polymer dynamics



A small colloidal particle in any liquid diffuses due to the fluctuations of the number of molecules hitting it randomly from different directions. Colloidal particles are significantly larger than the molecules in the liquid, but small enough that collisions with molecules noticeably move the particle.¹ The trajectory of the particle, shown in Fig. 8.1, is another example of a random walk. The three-dimensional mean-square displacement of the colloidal particle during time t is proportional to t , with the coefficient of proportionality related to the **diffusion coefficient** D :

$$\langle [\vec{r}(t) - \vec{r}(0)]^2 \rangle = 6Dt. \quad (8.1)$$

The average distance the particle has moved is proportional to the square root of time:

$$\langle [\vec{r}(t) - \vec{r}(0)]^2 \rangle^{1/2} = (6Dt)^{1/2}. \quad (8.2)$$

Whereas the motion of the particle obeys Eq. (8.1) at all times, we shall see that the motion of monomers in a polymer is not always described by Eq. (8.1) [or Eq. (8.2)]. When the motion of a molecule obeys Eq. (8.1), it is called a simple **diffusive motion**. The random motion of small particles in a liquid was observed long ago using a microscope by a biologist named Brown and is often referred to as **Brownian motion**.

If a constant force \vec{f} is applied to a small particle, pulling it through a liquid, the particle will achieve a constant velocity \vec{v} in the same direction as the applied force. For a given particle and a given liquid, the coefficient relating force and velocity is the **friction coefficient** ζ :

$$\vec{f} = \zeta \vec{v}. \quad (8.3)$$

Since the constant force acting on the particle results in a constant velocity, there must be an equal and opposite viscous drag force of the liquid acting on the particle with magnitude ζv . The diffusion coefficient D and the friction coefficient ζ are related through the **Einstein relation**:

$$D = \frac{kT}{\zeta}. \quad (8.4)$$

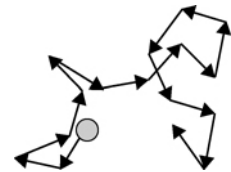


Fig. 8.1

Motion of a particle in a liquid is a random walk that results from random collisions with molecules in the liquid.

¹ Colloidal particles have sizes between 1 nm and 10 μm .

Unentangled polymer dynamics

The physics behind this relation is the fluctuation–dissipation theorem: the same random kicks of the surrounding molecules cause both Brownian diffusion and the viscous dissipation leading to the frictional force. It is instructive to calculate the time scale τ required for the particle to move a distance of order of its own size R :

$$\tau \approx \frac{R^2}{D} \approx \frac{R^2 \zeta}{kT}. \quad (8.5)$$

The time scale for diffusive motion is proportional to the friction coefficient.

The mechanical properties of a liquid are fundamentally different from the solids discussed in Chapter 7. Solids have stress proportional to deformation (for small deformations). However, the stress in liquids depends only on the rate of deformation, not the total amount of deformation. If we pour water from one bucket into another bucket, there is only resistance during the flow, but there is no shear stress in the water in either bucket at rest. We describe the deformation rate of a liquid in shear by the shear rate $\dot{\gamma} = d\gamma/dt$ [Eq. (7.99)]. For the steady simple shear flow of Fig. 7.23, the shear rate is the same everywhere, equal to the way in which velocity changes with vertical position. The stress σ in a Newtonian liquid is proportional to this shear rate [Newton’s law of viscosity Eq. (7.100), $\sigma = \eta\dot{\gamma}$], with the viscosity η being the coefficient of proportionality.

If a sphere of radius R moves in a Newtonian liquid of viscosity η , a simple dimensional argument can determine the friction coefficient of the sphere. The friction should depend only on the viscosity of the surrounding liquid and the sphere size:

$$\zeta(\eta, R). \quad (8.6)$$

The friction coefficient is the ratio of force and velocity, with units of kg s^{-1} . The viscosity is the ratio of stress and shear rate, with units of $\text{kg m}^{-1} \text{s}^{-1}$ and the sphere radius has units of length (m). The only functional form that is dimensionally correct gives a very simple relation:

$$\zeta \approx \eta R. \quad (8.7)$$

The full calculation of the slow flow of a Newtonian liquid past a sphere was published by Stokes in 1880, yielding the numerical prefactor of 6π that results in **Stokes law**:

$$\zeta = 6\pi\eta R. \quad (8.8)$$

Combining Stokes law with the Einstein relation [Eq. (8.4)] gives a simple equation for the diffusion coefficient of a spherical particle in a liquid, known as the **Stokes–Einstein relation**:

$$D = \frac{kT}{6\pi\eta R}. \quad (8.9)$$

This important relation is used to determine coil size from measured diffusion coefficient (for example, by dynamic light scattering—see Section 8.9, or by pulsed-field gradient NMR). The size determined from a measurement of diffusion coefficient is the **hydrodynamic radius**:

$$R_h \equiv \frac{kT}{6\pi\eta D}. \quad (8.10)$$

8.1 Rouse model

The first successful molecular model of polymer dynamics was developed by Rouse. The chain in the Rouse model is represented as N beads connected by springs of root-mean-square size b , as shown in Fig. 8.2. The beads in the Rouse model only interact with each other through the connecting springs. Each bead is characterized by its own independent friction with friction coefficient ζ . Solvent is assumed to be freely draining through the chain as it moves.

The total friction coefficient of the whole Rouse chain is the sum of the contributions of each of the N beads:

$$\zeta_R = N\zeta. \quad (8.11)$$

The viscous frictional force the chain experiences if it is pulled with velocity \vec{v} is $\vec{f} = -N\zeta\vec{v}$. The diffusion coefficient of the Rouse chain is obtained from the Einstein relation [Eq. (8.4)].

$$D_R = \frac{kT}{\zeta_R} = \frac{kT}{N\zeta}. \quad (8.12)$$

The polymer diffuses a distance of the order of its size during a characteristic time, called the **Rouse time**, τ_R :

$$\tau_R \approx \frac{R^2}{D_R} \approx \frac{R^2}{kT/(N\zeta)} = \frac{\zeta}{kT} NR^2. \quad (8.13)$$

The Rouse time has special significance. On time scales shorter than the Rouse time, the chain exhibits viscoelastic modes that shall be described in Section 8.4. However, on time scales longer than the Rouse time, the motion of the chain is simply diffusive.

Polymers are fractal objects, with size related to the number of monomers in the chain² by a power law:

$$R \approx bN^\nu \quad (8.14)$$

The reciprocal of the fractal dimension of the polymer (see Section 1.4) is ν . For an ideal linear chain $\nu = 1/2$ and the fractal dimension is $1/\nu = 2$. The Rouse time of such a fractal chain can be written as the product of

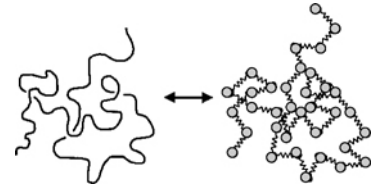


Fig. 8.2

In the Rouse model, a chain of N monomers is mapped onto a bead–spring chain of N beads connected by springs.

² There are $N - 1$ springs in the Rouse model and, for long chains, the number of springs is approximated by N .

Unentangled polymer dynamics

the time scale for motion of individual beads, the **Kuhn monomer relaxation time**

$$\tau_0 \approx \frac{\zeta b^2}{kT}, \quad (8.15)$$

and a power law in the number of monomers in the chain:

$$\tau_R \approx \frac{\zeta}{kT} NR^2 = \frac{\zeta b^2}{kT} N^{1+2\nu} \approx \tau_0 N^{1+2\nu}. \quad (8.16)$$

For an ideal linear chain, $\nu = 1/2$ and the Rouse time is proportional to the square of the number of monomers in the chain:

$$\tau_R \approx \tau_0 N^2. \quad (8.17)$$

The full calculation of the relaxation time of an ideal chain was published by Rouse in 1953, with a coefficient of $1/(6\pi^2)$:

$$\tau_R = \frac{\zeta b^2}{6\pi^2 kT} N^2. \quad (8.18)$$

This Rouse stress relaxation time is half of the end-to-end vector correlation time because stress relaxation is determined from a quadratic function of the amplitudes of normal modes (see Problem 8.36).

The time scale for motion of individual monomers τ_0 , is the time scale at which a monomer would diffuse a distance of order of its size b if it were not attached to the chain. In a polymer solution with solvent viscosity η_s , each monomer's friction coefficient is given by Stokes law [Eq. (8.8)]:

$$\zeta \approx \eta_s b. \quad (8.19)$$

The monomer relaxation time τ_0 and the chain relaxation time of the Rouse model τ_R can be rewritten in terms of the solvent viscosity η_s :

$$\tau_0 \approx \frac{\eta_s b^3}{kT}, \quad (8.20)$$

$$\tau_R \approx \frac{\eta_s b^3}{kT} N^2. \quad (8.21)$$

When probed on time scales smaller than τ_0 , the polymer essentially does not move and exhibits elastic response. On time scales longer than τ_R , the polymer moves diffusively and exhibits the response of a simple liquid. For intermediate time scales $\tau_0 < t < \tau_R$, the chain exhibits interesting viscoelasticity discussed in Section 8.4.1.

8.2 Zimm model

The viscous resistance imparted by the solvent when a particle moves through it arises from the fact that the particle must drag some of the surrounding solvent with it. The force acting on a solvent molecule at distance r from the particle becomes smaller as r increases, but only slowly (decaying roughly as $1/r$). This long-range force acting on solvent

(and other particles) that arises from motion of one particle is called **hydrodynamic interaction**. In the case of the bead–spring model of a polymer chain, when one bead moves, there are hydrodynamic interaction forces acting on the other beads of the chain. The Rouse model ignores hydrodynamic interaction forces, and assumes the beads only interact through the springs that connect them. We shall see later that this assumption is reasonable for polymer melts, but is not correct for a polymer in a dilute solution.

In dilute solutions, hydrodynamic interactions between the monomers in the polymer chain are strong. These hydrodynamic interactions also are strong between the monomers and the solvent within the pervaded volume of the chain. When the polymer moves, it effectively drags the solvent within its pervaded volume with it. For this reason, the best model of polymer dynamics in a dilute solution is the Zimm model, which effectively treats the pervaded volume of the chain as a solid object moving through the surrounding solvent.

Assume that the chain (and any section of the chain) drags with it the solvent in its pervaded volume. Thus the chain moves as a solid object of size $R \approx bN^\nu$. The friction coefficient of the chain of size R being pulled through a solvent of viscosity η_s is given by Stokes law:

$$\zeta_Z \approx \eta_s R. \quad (8.22)$$

There is a coefficient 6π in Stokes law [Eq. (8.8)] for a spherical object $\zeta = 6\pi\eta_s R$, but chains are not spheres and we drop all numerical coefficients.

From the Einstein relation [Eq. (8.4)] the diffusion coefficient of a chain in the Zimm model is reciprocally proportional to its size R :

$$D_Z = \frac{kT}{\zeta_Z} \approx \frac{kT}{\eta_s R} \approx \frac{kT}{\eta_s b N^\nu}. \quad (8.23)$$

This is simply the Stokes–Einstein relation [Eq. (8.9)] for a polymer in dilute solution. The Zimm model predicts that the chain diffuses as a particle with volume proportional to the chain's pervaded volume in solution. In 1956, Zimm published a full calculation, where he preaveraged the hydrodynamic interactions to obtain this result with an extra coefficient of $8/(3\sqrt{6}\pi^3)$ for an ideal chain:

$$D_Z = \frac{8}{3\sqrt{6}\pi^3} \frac{kT}{\eta_s R} \cong 0.196 \frac{kT}{\eta_s R}. \quad (8.24)$$

In the Zimm model, the chain diffuses a distance of order of its own size during the **Zimm time** τ_Z :

$$\tau_Z \approx \frac{R^2}{D_Z} \approx \frac{\eta_s}{kT} R^3 \approx \frac{\eta_s b^3}{kT} N^{3\nu} \approx \tau_0 N^{3\nu}. \quad (8.25)$$

The coefficient relating the relaxation time to a power of the number of monomers in the chain is once again the monomer relaxation time τ_0

Unentangled polymer dynamics

[Eq. (8.20)]. Zimm's full calculation of the chain relaxation time provides an extra coefficient of $1/(2\sqrt{3\pi})$ for an ideal chain:

$$\tau_Z = \frac{1}{2\sqrt{3\pi}} \frac{\eta_s}{kT} R^3 \cong 0.163 \frac{\eta_s}{kT} R^3. \quad (8.26)$$

This Zimm stress relaxation time is half of the Zimm end-to-end vector correlation time.

The Zimm time is proportional to the pervaded volume of the chain. Note that the Zimm time τ_Z has a weaker dependence on chain length than the Rouse time τ_R [Eq. (8.16)].

$$3\nu < 2\nu + 1 \quad \text{for } \nu < 1. \quad (8.27)$$

Comparison of Eqs (8.16) and (8.25) reveals that the Zimm time is shorter than the Rouse time in dilute solution. In principle, a chain in dilute solution could move a distance of order of its size by Rouse motion, by Zimm motion, or some combination of the two. The chain could simply move its monomers by Rouse motion through the solvent without dragging any of the solvent molecules with it, or it could drag all of the solvent in its pervaded volume with it, thereby moving by Zimm motion. In dilute solution, Zimm motion has less frictional resistance than Rouse motion, and therefore, the faster process is Zimm motion. The chain effectively moves as though it were a solid particle with volume of order of its pervaded volume (with linear size R). The solvent within the pervaded volume of the chain is hydrodynamically coupled to the chain.³ When the chain moves in response to its monomers being randomly hit by solvent from different directions, it effectively drags the surrounding solvent with it.

Using Eq. (3.77) for the size of the chain in a good solvent with intermediate excluded volume v in Eq. (8.25), and combining with the θ -solvent result of Eq. (8.25) with $\nu = 1/2$, yields a general expression for the Zimm time in dilute polymer solutions:

$$\tau_Z \approx \frac{\eta_s}{kT} R^3 \approx \begin{cases} \tau_0 N^{3/2} & N < b^6/v^2 \\ \tau_0 (v/b^3)^{6\nu-3} N^{3\nu} & N > b^6/v^2 \end{cases} \quad (8.28)$$

Using $\nu = 0.588$, the Zimm relaxation time for long chains is $\tau_0 (v/b^3)^{0.53} N^{1.76}$.

8.3 Intrinsic viscosity

In solution, a confusing plethora of viscosities have been defined over the years. The ratio of solution viscosity η to solvent viscosity η_s is the **relative viscosity**:

$$\eta_r \equiv \frac{\eta}{\eta_s}. \quad (8.29)$$

³ While some solvent does move with the chain, solvent molecules diffuse into and out of the pervaded volume on a faster time scale than the diffusion of the polymer (see Problem 8.5).

The relative viscosity is the simplest dimensionless measure of solution viscosity. The difference of the relative viscosity from unity is the **specific viscosity**:

$$\eta_{sp} \equiv \eta_r - 1 = \frac{\eta - \eta_s}{\eta_s}. \quad (8.30)$$

The numerator ($\eta - \eta_s$) is the polymer contribution to the solution viscosity, so the specific viscosity is a dimensionless measure of the polymer contribution to the solution viscosity.

The ratio of specific viscosity to polymer concentration is the **reduced viscosity**, η_{sp}/c , which has units of reciprocal concentration. In the limit of very low concentrations (far below the overlap concentration) the reduced viscosity becomes a very important material property called the intrinsic viscosity (see Section 1.7.3, and in particular Fig. 1.24):

$$[\eta] = \lim_{c \rightarrow 0} \frac{\eta_{sp}}{c}. \quad (8.31)$$

The intrinsic viscosity is the initial slope of specific viscosity as a function of concentration, and has units of reciprocal concentration [see Eq. (1.97)].

The value of the stress relaxation modulus at the relaxation time $G(\tau)$ is of the order of kT per chain in either the Rouse or Zimm models, just as the strands of a network in Chapter 7 stored of order kT of elastic energy:

$$G(\tau) \approx kT \frac{\phi}{Nb^3}. \quad (8.32)$$

The polymer contribution to the viscosity in either the Rouse or the Zimm model is proportional to $G(\tau)\tau$ [Eq. (7.120)]:

$$\eta - \eta_s \approx kT \frac{\phi}{Nb^3} \tau. \quad (8.33)$$

The typical experimental concentration used in defining intrinsic viscosity is the polymer mass per unit volume of solution, $c = \phi M_0 / (b^3 \mathcal{N}_{Av})$ where M_0 is the molar mass of a Kuhn monomer [see Eq. (1.18)]. The intrinsic viscosity then follows:

$$[\eta] \approx \frac{kT \mathcal{N}_{Av}}{\eta_s M_0 N} \tau. \quad (8.34)$$

The expression for the relaxation time in the Rouse model of an ideal chain $\tau_R \approx \eta_s b^3 N^2 / (kT)$ [Eq. (8.21)] leads to the Rouse prediction for the intrinsic viscosity:

$$[\eta] \approx \frac{b^3 \mathcal{N}_{Av}}{M_0} N \quad \text{Rouse model.} \quad (8.35)$$

The Rouse model predicts that the intrinsic viscosity in a θ -solvent is proportional to molar mass. However, the Rouse model assumes no

Unentangled polymer dynamics

hydrodynamic interactions and is not expected to be valid in dilute solutions where intrinsic viscosity is defined.

Substituting the prediction for the relaxation time of the Zimm model $\tau_Z \approx \eta_s R^3 / (kT)$ [Eq. (8.25)] into the expression for intrinsic viscosity [Eq. (8.34)] leads to the Zimm prediction for intrinsic viscosity:

$$[\eta] \approx \frac{R^3 \mathcal{N}_{Av}}{M_0 N} \approx \frac{b^3 \mathcal{N}_{Av}}{M_0} N^{3\nu-1} \quad \text{Zimm model.} \quad (8.36)$$

The Zimm model assumes that as the polymer moves it drags the solvent inside its pervaded volume with it. The Zimm model has the correct physics for the intrinsic viscosity. Equation (8.36) is more commonly written in terms of the molar mass $M = M_0 N$,

$$[\eta] = \Phi \frac{R^3}{M}, \quad (8.37)$$

where $\Phi = 0.425 \mathcal{N}_{Av} = 2.5 \times 10^{23} \text{ mol}^{-1}$ is a universal constant for all polymer–solvent systems. This famous relation between intrinsic viscosity, coil size and molar mass is known as the Fox–Flory equation.

Equation (8.36) predicts that the intrinsic viscosity obeys a power law in molar mass. This power law was empirically recognized long ago, and is known as the Mark–Houwink equation [Eq. (1.100)]:

$$[\eta] = KM^a. \quad (8.38)$$

From the derivation of the Fox–Flory equation, based on the Zimm model, the Mark–Houwink exponent a is related to the exponent describing the molar mass dependence of coil size in solution ν :

$$a = 3\nu - 1. \quad (8.39)$$

The Mark–Houwink equation provides an indirect estimate of molar mass from a measurement of intrinsic viscosity $[\eta]$, if the two Mark–Houwink constants K and a , are known. The predictions of Mark–Houwink constants are summarized in Table 8.1. Comparison with Table 1.4 shows that the Zimm model agrees reasonably well with experimental results, as $a = 0.50$ is observed in θ -solvent and $0.7 < a < 0.8$ is usually observed in good solvents.

Using the Zimm time [Eq. (8.28)] in Eq. (8.34), yields a general expression for the intrinsic viscosity, valid for any solvent with $T \geq \theta$:

$$\begin{aligned} [\eta] &\approx \frac{kT \mathcal{N}_{Av}}{\eta_s M_0 N} \tau_Z \approx \frac{R^3 \mathcal{N}_{Av}}{M_0 N} \\ &\approx \frac{b^3 \mathcal{N}_{Av}}{M_0} \begin{cases} N^{1/2} & N < b^6 / v^2 \\ (v/b^3)^{6\nu-3} N^{3\nu-1} & N > b^6 / v^2 \end{cases} \end{aligned} \quad (8.40)$$

Table 8.1 Predictions of Mark–Houwink constants

	K	a
Rouse model in θ -solvent	$b^3 \mathcal{N}_{Av} / M_0^2$	1
Zimm model in θ -solvent	$b^3 \mathcal{N}_{Av} / M_0^{3/2}$	$3\nu - 1 = 1/2$
Zimm model in good solvent	$b^3 \mathcal{N}_{Av} / M_0^{1.764}$	$3\nu - 1 \approx 0.76$

For long chains in good solvent, $\nu = 0.588$ and the intrinsic viscosity *universally* scales as $\nu^{0.53} N^{0.76}$.

This relation is tested with experimental data in Fig. 8.3.⁴ It is important to point out the fact that the intrinsic viscosity of polystyrene in toluene (filled squares in Fig. 8.3) crosses over to the θ -solvent result at $M \approx 30\,000 \text{ g mol}^{-1}$. This provides a direct measure of the number of Kuhn monomers in a thermal blob $g_T \approx (30\,000 \text{ g mol}^{-1}) / (720 \text{ g mol}^{-1}) \approx 40$ for polystyrene in toluene. The crossover between the θ -solvent and good solvent cases of Eq. (8.40) is at $N = g_T \approx (b^3/\nu)^2$ [Eq. (3.75)], so $g_T \approx 40$ means that the excluded volume is estimated to be $\nu \approx 0.16b^3$ for polystyrene in toluene. Hence, although toluene is a quite good solvent for polystyrene, it is nowhere near the athermal solvent limit, which would have even higher intrinsic viscosity that would maintain the power law with 0.76 slope to even lower molar masses. Polystyrene in methyl ethyl ketone (open circles in Fig. 8.3) has even smaller excluded volume, as $g_T \approx (100\,000 \text{ g mol}^{-1}) / (720 \text{ g mol}^{-1}) \approx 140$ and $\nu \approx 0.08b^3$.

Figure 8.3 also shows clearly that caution is needed when using Mark–Houwink equations from the literature that have intermediate exponents in the range $0.5 < a < 0.76$. Such intermediate exponents correspond to the crossover between regimes and are only valid for the range of molar masses they were measured in.

The fact that the intrinsic viscosity measurement is simultaneously simple and precise makes it an extremely popular molecular characterization tool. Intrinsic viscosity can easily be measured to $\pm 0.1\%$ precision, which is far superior to osmotic pressure and light scattering, which have precisions of $\pm 5\%$ under the best of circumstances. Furthermore, if intrinsic viscosity and absolute molar mass are measured over a sufficiently wide range, the thermodynamic nature of the polymer solvent interaction, reflected in the excluded volume ν , can be estimated using Eq. (8.40).

The temperature dependence of intrinsic viscosity enters Eq. (8.40) through the excluded volume $\nu \approx b^3 (T - \theta) / T$. For chains that are smaller than the thermal blob, the short chain branch of Eq. (8.40) (with $N < b^6/\nu^2$) applies. For such short chains, the intrinsic viscosity is independent of temperature and $[\eta] / N^{1/2}$ reduces data for different lengths of short chains to a common temperature-independent line, demonstrated in Fig. 8.4(a) for polyisobutylene in toluene with $M < 11\,000 \text{ g mol}^{-1}$. On the other hand, chains with size far exceeding the thermal blob size have important excluded volume effects. The long chain branch of Eq. (8.40) (with $N > b^6/\nu^2$) applies to long chains and $[\eta] / N^{0.764}$ reduces data for different lengths of long chains to a common curve, as shown in Fig. 8.4(b) for polyisobutylene in toluene with $M > 400\,000 \text{ g mol}^{-1}$. The curve in Fig. 8.4(b) is determined by the temperature dependence of excluded volume $(\nu/b^3)^{0.53} \approx (1 - \theta/T)^{0.53}$ with $\theta = 245 \text{ K} \approx -28^\circ\text{C}$ determined from the fit. Intermediate molar masses (not shown) with $M = 48\,000 \text{ g mol}^{-1}$ and

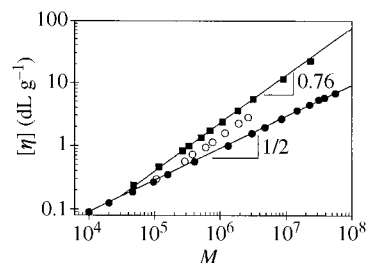
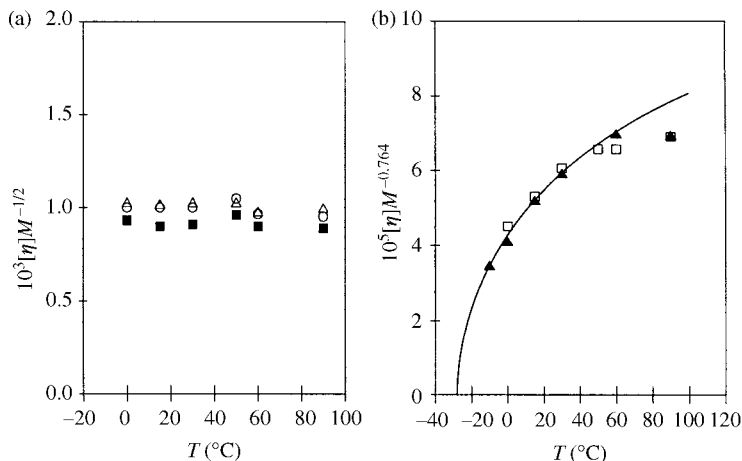


Fig. 8.3

Intrinsic viscosities of polystyrenes in three solvents. Cyclohexane is a θ -solvent ($\nu = 0$, filled circles, from Y. Einaga *et al.*, *J. Polym. Sci., Polym. Phys.* **17**, 2103, 1979), with Mark–Houwink exponent $a = 1/2$. Methyl ethyl ketone is a better solvent ($\nu \approx 0.08b^3$, open circles, from R. Okada *et al.*, *Makromol. Chem.* **59**, 137, 1963) and toluene is a good solvent ($\nu \approx 0.16b^3$, filled squares, from R. Kniewske and W.-M. Kulicke, *Makromol. Chem.* **184**, 2173, 1983) with $a = 0.76$.

⁴ The customary units for intrinsic viscosity are dL g^{-1} , where $1 \text{ dL} = 0.1 \text{ L}$.

Unentangled polymer dynamics

**Fig. 8.4**

Temperature dependence of intrinsic viscosity for polyisobutylene fractions in toluene. (a) data for the three lowest molar masses (open triangles are $M = 7080 \text{ g mol}^{-1}$, filled squares are $M = 9550 \text{ g mol}^{-1}$ and open circles are $M = 10\,200 \text{ g mol}^{-1}$) that all are smaller than the thermal blob and hence have unperturbed size. The short chain branch of Eq. (8.40) reduces these data to a common temperature-independent line. (b) data for the two highest molar masses (open squares are $M = 463\,000 \text{ g mol}^{-1}$ and filled triangles are $M = 1\,260\,000 \text{ g mol}^{-1}$) that obey the long chain branch of Eq. (8.40). The curve is fitted to the data using Eq. (8.40) and the temperature dependence of excluded volume with $\theta = -28^\circ\text{C}$ determined from the fit. The data are from T. G. Fox and P. J. Flory, *J. Phys. Chem.* **53**, 197 (1949).

$M = 110\,000 \text{ g mol}^{-1}$ fall in the crossover between the two limiting cases of Eq. (8.40) and do not obey the scaling of either clean limit. Unfortunately, the molar mass range of $20\,000 < M < 200\,000 \text{ g mol}^{-1}$ is the important range for commercial polymers, and it corresponds to the crossover for most good solvent/polymer solutions.

The R^3 in Eq. (8.37) comes from the relaxation time in Eq. (8.34). This Zimm time really has two size scales within it. The hydrodynamic radius R_h enters through the diffusion coefficient [Eq. (8.10)] and the radius of gyration R_g enters through the length scale that the molecule moves in its relaxation time:

$$[\eta] \approx \frac{\mathcal{R}T}{\eta_s M} \tau_Z \approx \frac{\mathcal{R}T R_g^2}{\eta_s M D_Z} \approx \frac{\mathcal{N}_{\text{Av}} R_g^2 R_h}{M}. \quad (8.41)$$

Using data for polystyrene in two good solvents⁵ (ethylbenzene and tetrahydrofuran) Eq. (8.41) is found to apply reasonably with

$$\frac{[\eta] M_w}{\mathcal{N}_{\text{Av}} R_g^2 R_h} \cong 7, \quad (8.42)$$

in the range $93\,000 \text{ g mol}^{-1} \leq M_w \leq 4\,800\,000 \text{ g mol}^{-1}$.

⁵ K. Venkataswamy *et al.*, *Macromolecules* **19**, 124 (1986).

8.4 Relaxation modes

In Sections 8.1 and 8.2, we calculated the longest relaxation time of unentangled polymers using molecular models. The linear viscoelastic response of polymeric liquids, discussed in Section 7.6, measures the full spectrum of relaxation times. Since polymer chains are self-similar objects, they also exhibit dynamic self-similarity. *Smaller sections of a polymer chain with g monomers relax just like a whole polymer chain that has g monomers.* In all unentangled molecular models for polymer dynamics (both Rouse and Zimm and combinations thereof) the relaxations are described by N different **relaxation modes**. The modes are numbered by **mode index** $p = 1, 2, 3, \dots, N$. These modes are analogous to the modes of a vibrating guitar string. Mode p involves coherent motion of sections of the whole chain with N/p monomers, and the corresponding relaxation time of this mode τ_p is similar to the longest relaxation time of a chain with N/p monomers. For all unentangled molecular models of flexible polymer dynamics, the shortest mode has mode index $p = N$ with relaxation time τ_0 , the relaxation time of a monomer [Eq. (8.20)]. The longer modes depend on whether hydrodynamic interactions are important or not, as discussed below.

Consider a polymer liquid subjected to a unit step strain at time $t = 0$. The **equipartition principle** states that $kT/2$ of free energy is associated with each degree of freedom at equilibrium.⁶ Immediately following the unit step strain, the entire chain stores of order NkT of elastic energy, since there are N independent modes that each store of order kT . To determine the time dependent viscoelastic response, we simply need to determine the relaxation time of each mode.

8.4.1 Rouse modes

In the Rouse model, the (longest) relaxation time of the ideal chain is given by Eq. (8.17):

$$\tau_R \approx \tau_0 N^2. \quad (8.43)$$

Since the p th mode involves relaxation on the scale of chain sections with N/p monomers, the relaxation time of the p th mode has a similar form to the longest mode:

$$\tau_p \approx \tau_0 \left(\frac{N}{p} \right)^2 \quad \text{for } p = 1, 2, \dots, N. \quad (8.44)$$

The relaxation time of a monomer, τ_0 [Eq. (8.15)] is the shortest relaxation time of the Rouse model, with mode index $p = N$, making $\tau_N = \tau_0$. The mode with index $p = 1$ is the longest relaxation mode of the chain with relaxation time equal to the Rouse time $\tau_1 = \tau_R$, and corresponds to relaxation on the scale of the entire chain. The mode with index $p = 2$ corresponds to the two halves of the chain with $N/2$ monomers, each

⁶ In three-dimensional space, each mode has three degrees of freedom.

Unentangled polymer dynamics

relaxing independently. The mode with index p breaks the chain into p sections of N/p monomers, and each of these sections relax as independent chains of N/p monomers on the time scale τ_p .

As expected, higher index modes, involving fewer monomers, relax faster than lower index modes. Therefore, at time τ_p after a step strain, all modes with index higher than p have mostly relaxed, but modes with index lower than p have not yet relaxed.

The number of unrelaxed modes per chain at time $t = \tau_p$ is equal to the mode index p . Each unrelaxed mode contributes energy of order kT to the stress relaxation modulus. The stress relaxation modulus at time $t = \tau_p$ is proportional to the thermal energy kT and the number density of sections with N/p monomers, $\phi/(b^3 N/p)$:

$$G(\tau_p) \approx \frac{kT \phi}{b^3 N} p. \quad (8.45)$$

The time dependence of the mode index p for the mode that relaxes at time $t = \tau_p$ can be found from Eq. (8.44).

$$p \approx \left(\frac{\tau_p}{\tau_0} \right)^{-1/2} N. \quad (8.46)$$

Combining Eqs (8.45) and (8.46) approximates the stress relaxation modulus for the Rouse model at intermediate time scales:

$$G(t) \approx \frac{kT}{b^3} \phi \left(\frac{t}{\tau_0} \right)^{-1/2} \quad \text{for } \tau_0 < t < \tau_R. \quad (8.47)$$

This expression effectively interpolates between a modulus level of order kT per monomer at the shortest Rouse mode ($t \approx \tau_0$) to a modulus level of order kT per chain at the longest Rouse mode ($t = \tau_R \approx \tau_0 N^2$) using a power law. We already know that the stress relaxation modulus has an exponential decay beyond its longest relaxation time [Eq. (7.112)]. Therefore, an approximate description of the stress relaxation modulus of the Rouse model is the product of [Eq. (8.47)] and an exponential cutoff:

$$G(t) \approx \frac{kT}{b^3} \phi \left(\frac{t}{\tau_0} \right)^{-1/2} \exp(-t/\tau_R) \quad \text{for } t > \tau_0. \quad (8.48)$$

The Rouse time τ_R is the longest stress relaxation time [Eq. (8.18)].

For oscillatory shear, Eqs (7.149) and (7.150) allow calculation of the storage and loss moduli of a solution of linear Rouse chains (see Problem 8.14):

$$G'(\omega) \approx \frac{\phi kT}{b^3 N} \frac{(\omega \tau_R)^2}{\sqrt{[1 + (\omega \tau_R)^2]} \sqrt{1 + (\omega \tau_R)^2 + 1}} \quad \text{for } \omega < 1/\tau_0, \quad (8.49)$$

$$G''(\omega) \approx \frac{\phi kT}{b^3 N} \omega \tau_R \sqrt{\frac{\sqrt{1 + (\omega \tau_R)^2} + 1}{1 + (\omega \tau_R)^2}} \quad \text{for } \omega < 1/\tau_0. \quad (8.50)$$

In the frequency range, $1/\tau_R \ll \omega \ll 1/\tau_0$, the storage and loss moduli of the Rouse model are equal to each other and scale as the square root of frequency:

$$G'(\omega) \cong G''(\omega) \sim \omega^{1/2} \quad \text{for } 1/\tau_R \ll \omega \ll 1/\tau_0. \quad (8.51)$$

For high frequencies $\omega > 1/\tau_0$, there are no relaxation modes in the Rouse model. The storage modulus becomes independent of frequency, and equal to the short time stress relaxation modulus, which is kT per monomer $G'(\omega) \approx \phi kT/b^3$. This high-frequency saturation is not included in Eqs (8.49) and (8.50). At low frequencies $\omega < 1/\tau_R$, the storage modulus is proportional to the square of frequency and the loss modulus is proportional to frequency, as is the case for the terminal response of any viscoelastic liquid.

Figure 8.5 shows that experimental data on unentangled polyelectrolyte solutions are described quite well by the Rouse model. Polyelectrolytes are charged polymers that have a wide range of concentrations where dynamics obey the Rouse model.

The viscosity of the Rouse model is obtained by integrating $G(t)$ [Eq. (7.117)]:

$$\begin{aligned} \eta &= \int_0^\infty G(t) dt \approx \frac{kT}{b^3} \phi \int_0^\infty \left(\frac{t}{\tau_0}\right)^{-1/2} \exp(-t/\tau_R) dt \\ &\approx \frac{kT}{b^3} \phi \sqrt{\tau_0 \tau_R} \int_0^\infty x^{-1/2} \exp(-x) dx \approx \frac{kT}{b^3} \phi \sqrt{\tau_0 \tau_R} \approx \frac{kT}{b^3} \tau_0 N \phi \approx \frac{\zeta}{b} N \phi. \end{aligned} \quad (8.52)$$

Equation (8.52) made use of the variable transformation $x \equiv t/\tau_R$, and the integral involving x is simply a numerical coefficient. Notice that the final relation is identical to that expected by Eq. (7.120), the product of $G(\tau_R)$ [Eq. (8.32)] and τ_R [Eq. (8.17)]. The Rouse model applies to melts of short unentangled chains (for which hydrodynamic interactions are screened). The Rouse viscosity has a very simple form for an unentangled polymer melt:

$$\eta \approx \frac{\zeta}{b} N. \quad (8.53)$$

The viscosity of the Rouse model is proportional to the number of monomers in the chain. The Rouse model has been solved exactly (by Rouse), and the full calculation gives an extra coefficient of 1/36:

$$\eta = \frac{\zeta}{36b} N. \quad (8.54)$$

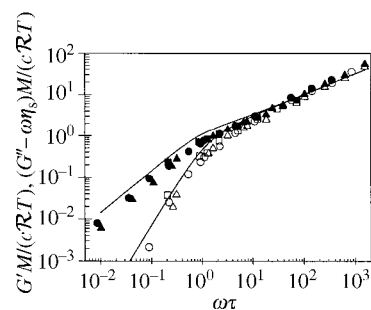


Fig. 8.5

Oscillatory shear data for solutions of poly(2-vinyl pyridine) in 0.0023 M HCl in water. Open symbols are the storage modulus G' and filled symbols are the loss modulus G'' . Squares have $c = 0.5 \text{ g L}^{-1}$, triangles have $c = 1.0 \text{ g L}^{-1}$, and circles have $c = 2.0 \text{ g L}^{-1}$. The curves are the predictions of the Rouse model [Eqs (8.49) and (8.50)]. Data from D. F. Hodgson and E. J. Amis, *J. Chem. Phys.* **94**, 4581 (1991).

Unentangled polymer dynamics

Rouse also derived an exact relation for the stress relaxation modulus,

$$G(t) = kT \frac{\phi}{Nb^3} \sum_{p=1}^N \exp(-t/\tau_p), \quad (8.55)$$

with

$$\tau_p = \frac{\zeta b^2 N^2}{6\pi^2 kT p^2}. \quad (8.56)$$

The stress relaxation times τ_p of the Rouse model are half of the correlation times of normal modes (see Problem 8.36).

This exact form demonstrates that each mode ($p = 1, 2, \dots, N$) relaxes as a Maxwell element [Eq. (7.111)]. The exact [Eq. (8.55)] and approximate [Eq. (8.48)] Rouse predictions of the stress relaxation modulus of an unentangled polymer melt are compared in Fig. 8.6. This figure clearly shows that Eq. (8.48) is an excellent approximation of the exact Rouse result for long chains ($N \gg 1$).

Chain sections containing N/p monomers move a distance of order of their size $b(N/p)^{1/2}$ during the mode relaxation time τ_p . The position vector of monomer j at time t is $\vec{r}_j(t)$. The mean-square displacement of monomer j during time τ_p is of the order of the mean-square size of the sections involved in coherent motion on this time scale:

$$\langle [\vec{r}_j(\tau_p) - \vec{r}_j(0)]^2 \rangle \approx b^2 \frac{N}{p} \approx b^2 \left(\frac{\tau_p}{\tau_0} \right)^{1/2}. \quad (8.57)$$

In the final relation we used the time dependence of the mode index p [Eq. (8.46)]. The mean-square displacement of a monomer on intermediate time scales thus increases as the square root of time:

$$\langle [\vec{r}_j(t) - \vec{r}_j(0)]^2 \rangle \approx b^2 \left(\frac{t}{\tau_0} \right)^{1/2} \quad \text{for } \tau_0 < t < \tau_R. \quad (8.58)$$

For the motion to be diffusive, the mean-square displacement must be linear in time [see Eq. (8.1)]. Since the mean-square displacement on intermediate time scales is a weaker-than-linear power of time, the motion is referred to as **subdiffusive motion**. Individual monomers are not ‘aware’ that they belong to an N -mer on times shorter than the Rouse time of the chain. At each moment of time $t < \tau_R$, sections of a chain containing $g(t)$ monomers move coherently. Thus monomers only ‘realize’ that their chain contains at least $g(t)$ monomers at time scale $t < \tau_R$. The diffusion coefficient of these coherent sections is $D(t) \approx kT/(\zeta g)$. The number of monomers in sections that coherently participate in Rouse motion increases proportional to the square root of time $g(t) \approx (t/\tau_0)^{1/2}$ [Eq. (8.46) with $g = N/p$] and their effective diffusion coefficient decreases with time:

$$D(t) \approx \frac{kT}{\zeta g(t)} \approx \frac{kT}{\zeta} \left(\frac{t}{\tau_0} \right)^{-1/2} \quad \text{for } \tau_0 < t < \tau_R. \quad (8.59)$$

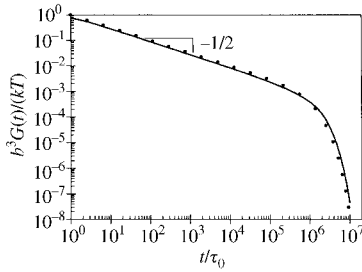


Fig. 8.6

Stress relaxation modulus predicted by the Rouse model for a melt of unentangled chains with $N = 10^3$. The solid curve is the exact Rouse result [Eq. (8.55)] and the dotted curve is the approximate Rouse result [Eq. (8.48)].

At longer times, monomers participate in collective motion of larger sections with smaller effective diffusion coefficient $D(t)$. Therefore the mean-square displacement of monomers is not a linear function of time, but instead subdiffusive:

$$\langle [\bar{r}_j(t) - \bar{r}_j(0)]^2 \rangle \approx D(t)t \sim t^{1/2} \quad \text{for } \tau_0 < t < \tau_R. \quad (8.60)$$

Only on time scales longer than the Rouse time of the chain, is the motion of the chain diffusive, with mean-square displacement proportional to time [Eq. (8.1)].

8.4.2 Zimm modes

Similar scaling analysis of the mode structure can be applied to the Zimm model. The relaxation time of the p th mode is of the order of the Zimm relaxation time of the chain containing N/p monomers [Eq. (8.25)]:

$$\tau_p \approx \tau_0 \left(\frac{N}{p} \right)^{3\nu}. \quad (8.61)$$

The index p of the mode relaxing at time $t = \tau_p$ after a step strain imposed at time $t = 0$ is obtained by solving the above equation for p :

$$p \approx N \left(\frac{\tau_p}{\tau_0} \right)^{-1/(3\nu)} = N \left(\frac{t}{\tau_0} \right)^{-1/(3\nu)}. \quad (8.62)$$

The number of unrelaxed modes per chain at time $t = \tau_p$ is p . The stress relaxation modulus is proportional to the number density of chain sections with N/p monomers:

$$G(t) \approx \frac{kT}{b^3} \frac{\phi}{N} p \approx \frac{kT}{b^3} \phi \left(\frac{t}{\tau_0} \right)^{-1/(3\nu)} \quad \text{for } \tau_0 < t < \tau_Z. \quad (8.63)$$

In θ -solvents ($\nu = 1/2$), the stress relaxation modulus decays as the $-2/3$ power of time, while in good solvents ($\nu \cong 0.588$) $G(t)$ decays approximately as the -0.57 power of time. Like the stress relaxation modulus of the Rouse model [Eq. (8.47)], Eq. (8.63) crosses over from kT per monomer at the monomer relaxation time τ_0 to kT per chain at the relaxation time of the chain $\tau_Z \approx \tau_0 N^{3\nu}$ [Eq. (8.25)]. Once again, an excellent approximation to the stress relaxation modulus predicted by the Zimm model is the product of the power law of Eq. (8.63) and an exponential cutoff:

$$G(t) \approx \frac{kT}{b^3} \phi \left(\frac{t}{\tau_0} \right)^{-1/(3\nu)} \exp(-t/\tau_Z) \quad \text{for } t > \tau_0. \quad (8.64)$$

The polymer contribution to the solution viscosity is obtained by integrating $G(t)$ [Eq. (7.117)]:

$$\begin{aligned}\eta - \eta_s &= \int_0^\infty G(t) dt \approx \frac{kT}{b^3} \phi \int_0^\infty \left(\frac{t}{\tau_0}\right)^{-1/3\nu} \exp(-t/\tau_Z) dt \\ &\approx \frac{kT}{b^3} \phi \tau_Z \left(\frac{\tau_Z}{\tau_0}\right)^{-1/3\nu} \int_0^\infty x^{-1/3\nu} \exp(-x) dx \approx \frac{kT}{b^3} \phi \tau_0 N^{3\nu-1} \\ &\approx \eta_s \phi N^{3\nu-1}.\end{aligned}\quad (8.65)$$

The variable transformation $x \equiv t/\tau_Z$ was used, and the integral involving x is simply a numerical coefficient. The second-to-last relation was obtained using $\tau_Z \approx \tau_0 N^{3\nu}$ [Eq. (8.25)] and the final relation used Eq. (8.20). The final relation is identical to that expected by Eq. (7.120), the product of $G(\tau_Z)$ [Eq. (8.32)] and τ_Z [Eq. (8.25)]. The Zimm model applies to the relaxation of the entire chain in dilute solution (where hydrodynamic interactions dominate). The intrinsic viscosity is calculated from the polymer contribution to the solution viscosity using Eq. (8.31) and the relation between mass concentration and volume fraction $c = \phi M_0 / (b^3 \mathcal{N}_{Av})$ [(see Eq. (1.18)]:

$$[\eta] = \lim_{c \rightarrow 0} \frac{\eta - \eta_s}{\eta_s c} \approx \frac{b^3 \mathcal{N}_{Av}}{M_0} N^{3\nu-1} \approx \frac{R^3 \mathcal{N}_{Av}}{M}.\quad (8.66)$$

This result is identical to Eqs (8.36) and (8.37), derived previously.

Using Eqs (7.149) and (7.150) with the approximate Zimm model prediction for the stress relaxation modulus [Eq. (8.64)] provides predictions of the storage and loss moduli that are valid for dilute solutions of linear chains (see Problem 8.16):

$$G'(\omega) \approx \frac{\phi k T \omega \tau_Z \sin [(1 - 1/(3\nu)) \arctan(\omega \tau_Z)]}{b^3 N [1 + (\omega \tau_Z)^2]^{(1-1/(3\nu))/2}},\quad (8.67)$$

$$G''(\omega) \approx \frac{\phi k T \omega \tau_Z \cos [(1 - 1/(3\nu)) \arctan(\omega \tau_Z)]}{b^3 N [1 + (\omega \tau_Z)^2]^{(1-1/(3\nu))/2}}.\quad (8.68)$$

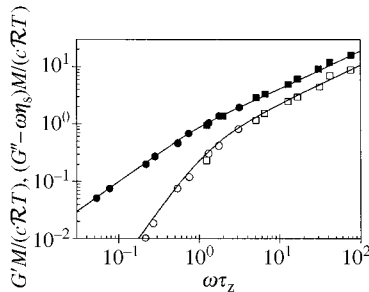


Fig. 8.7

Oscillatory shear data on dilute solutions of polystyrene with $M = 860\,000 \text{ g mol}^{-1}$ in two θ -solvents (circles are in decalin at 16°C and squares are in di-2-ethylhexyl phthalate at 22°C). Open symbols are the dimensionless storage modulus and filled symbols are the dimensionless loss modulus, both extrapolated to zero concentration. The curves are the predictions of the Zimm model [Eqs (8.67) and (8.68)]. Data from R. M. Johnson *et al.*, *Polym. J.* **1**, 742 (1970).

These predictions of the Zimm model are compared with experimental data on dilute polystyrene solutions in two θ -solvents in Fig. 8.7. The Zimm model gives an excellent description of the viscoelasticity of dilute solutions of linear polymers.

As in the Rouse model, the mean-square displacement of monomer j during time τ_p is of the order of the mean-square size of the section containing N/p monomers involved in a coherent motion at this time:

$$\langle [\vec{r}_j(\tau_p) - \vec{r}_j(0)]^2 \rangle \approx b^2 \left(\frac{N}{p}\right)^{2\nu} \approx b^2 \left(\frac{\tau_p}{\tau_0}\right)^{2/3}.\quad (8.69)$$

The time dependence of mode index p [Eq. (8.62)] was used to get the final result. Notice that this final result has an exponent that does not depend on

solvent quality. The mean-square displacement of a monomer in the Zimm model is subdiffusive on intermediate time scales:

$$\langle [\vec{r}_j(t) - \vec{r}_j(0)]^2 \rangle \approx b^2 \left(\frac{t}{\tau_0} \right)^{2/3} \quad \text{for } \tau_0 < t < \tau_Z. \quad (8.70)$$

Consistent with the fact that the longest relaxation time of the Zimm model is shorter than the Rouse model, the subdiffusive monomer motion of the Zimm model [(Eq. (8.70))] is always faster than in the Rouse model [Eq. (8.58)] with the same monomer relaxation time τ_0 . This is demonstrated in Fig. 8.8, where the mean-square monomer displacements predicted by the Rouse and Zimm models are compared. Each model exhibits subdiffusive motion on length scales smaller than the size of the chain, but motion becomes diffusive on larger scales, corresponding to times longer than the longest relaxation time.

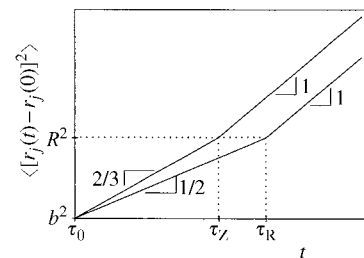


Fig. 8.8

Time dependence of the mean-square monomer displacements predicted by the Rouse and Zimm models on logarithmic scales.

8.5 Semidilute unentangled solutions

There are two limits for unentangled polymer dynamics:

(1) The Zimm limit applies to dilute solutions, where the solvent within the pervaded volume of the polymer is hydrodynamically coupled to the polymer. Polymer dynamics are described by the Zimm model in dilute solutions.

(2) The Rouse limit applies to unentangled polymer melts because hydrodynamic interactions are screened in melts (just as excluded volume interactions are screened in melts). Polymer dynamics in the melt state (with no solvent) are described by the Rouse model, for short chains that are not entangled.

In semidilute solutions there is a length scale, called the **hydrodynamic screening length** ξ_h , separating these two types of dynamics. On length scales shorter than the hydrodynamic screening length (for $r < \xi_h$), the hydrodynamic interactions dominate and dynamics are described by the Zimm model. On length scales larger than the screening length (for $r > \xi_h$) the hydrodynamic interactions are screened by surrounding chains and the dynamics are described by the Rouse model.

In Section 5.3, the static correlation length ξ was defined for semidilute solutions. This correlation length separates single-chain (dilute-like) conformations at shorter length scales ($r < \xi$) from many-chain (melt-like) statistics at longer length scales (for $r > \xi$). The concentration correlation blob of size ξ contains g monomers of a chain, with conformation similar to dilute solutions:

$$\xi \approx bg^\nu. \quad (8.71)$$

The exponent $\nu = 1/2$ in θ -solvents and $\nu \approx 0.588$ in good solvents. The correlation volumes are densely packed, so the volume fraction within

Unentangled polymer dynamics

each correlation volume (gb^3/ξ^3) must be the same as the overall volume fraction of the solution ϕ :

$$\phi \approx \frac{gb^3}{\xi^3}. \quad (8.72)$$

The correlation length decreases with increasing concentration [Eq. (5.23)]:

$$\xi \approx b\phi^{-\nu/(3\nu-1)}. \quad (8.73)$$

The scaling exponent $\nu/(3\nu-1) = 1$ in θ -solvents ($\nu = 1/2$) and $\nu/(3\nu-1) \cong 0.76$ in good solvents ($\nu \cong 0.588$).

The hydrodynamic screening length ξ_h in semidilute solutions is expected to be proportional to the static correlation length⁷ ξ :

$$\xi_h \approx \xi. \quad (8.74)$$

This proportionality makes sense in both limits. In the melt ($\phi = 1$), both excluded volume and hydrodynamic interactions are fully screened to the level of individual monomers, so $\xi_h \approx \xi \approx b$. At the overlap concentration ($\phi = \phi^*$), both excluded volume and hydrodynamic interactions apply over length scales comparable to the size of the entire chain, with $\xi_h \approx \xi \approx R$.

The hydrodynamic screening length can neither be much larger nor much smaller than the static correlation length. Each of the N modes of a chain can, in principle, relax by either Rouse or Zimm motion. On small length scales, Zimm modes are faster than Rouse modes (see Fig. 8.8) because only solvent and other monomers on the same chain are hydrodynamically coupled. However, this situation changes beyond the correlation length, because Zimm motion would couple the motion of monomers from different chains. This extra coupling makes Rouse motion faster than Zimm motion for sections of chain that are larger than the static correlation length, so Rouse dynamics apply on larger length scales.

In semidilute solutions, both statics and dynamics are similar to dilute solutions on length scales shorter than the screening length. For short distances from a given monomer ($r < \xi$), essentially all other monomers are from the same chain (see Fig. 5.4). The chain conformation is similar to dilute solution and the dynamics are controlled by strong hydrodynamic interactions. Therefore, the relaxation time τ_ξ of a chain section of size ξ is described by the Zimm model and proportional to the correlation volume ξ^3 :

$$\tau_\xi \approx \frac{\eta_s}{kT} \xi^3 \approx \frac{\eta_s b^3}{kT} \phi^{-3\nu/(3\nu-1)}. \quad (8.75)$$

On length scales larger than the screening length ξ the dynamics are many-chain-like, with both excluded volume and hydrodynamic interactions

⁷ Experimental results appear to be consistent with the expectation that hydrodynamic interactions and excluded volume interactions are screened on similar length scales.

screened. The Rouse model applies to the random walk chain of N/g correlation blobs. The relaxation time of the whole chain τ_{chain} is given by Eq. (8.17), with τ_{ξ} the effective ‘monomer’ relaxation time, N/g the effective number of ‘monomers’:

$$\tau_{\text{chain}} \approx \tau_{\xi} \left(\frac{N}{g} \right)^2 \approx \frac{\eta_s}{kT} \xi^3 \left(\frac{N}{g} \right)^2. \quad (8.76)$$

The number of monomers in a correlation blob is determined by combining Eqs (8.72) and (8.73) [as was done previously in deriving Eq. (5.24)]:

$$g \approx \phi \left(\frac{\xi}{b} \right)^3 \approx \phi^{-1/(3\nu-1)}. \quad (8.77)$$

From Eqs (8.76) and (8.77), the concentration dependence of the relaxation time of the chain in semidilute solution is obtained:

$$\tau_{\text{chain}} \approx \frac{\eta_s b^3}{kT} N^2 \phi^{(2-3\nu)/(3\nu-1)}. \quad (8.78)$$

The concentration dependence of the polymer’s relaxation time is a power law with exponent

$$\frac{2-3\nu}{3\nu-1} = 1 \quad \text{in } \theta \text{ - solvents } (\nu = 1/2), \quad (8.79)$$

and

$$\frac{2-3\nu}{3\nu-1} \cong 0.31 \quad \text{in good solvents } (\nu \cong 0.588). \quad (8.80)$$

Note that if the polymer in dilute solution were highly extended with exponent $\nu > 2/3$, the relaxation time in unentangled semidilute solutions would be predicted to *decrease* with increasing concentration. This is actually observed for semidilute unentangled solutions of charged polymers, called polyelectrolytes, which have $\nu = 1$ in dilute solutions because of charge repulsion. However, for the neutral flexible polymers discussed here, the relaxation time of the chain always increases with concentration.

Polymers diffuse a distance of the order of their size R during their relaxation time τ_{chain} . Recall the size of a linear polymer chain in a semidilute solution [Eq. (5.26) with $v = b^3$]:

$$R \approx \xi \left(\frac{N}{g} \right)^{1/2} \approx b N^{1/2} \phi^{-(2\nu-1)/(6\nu-2)}. \quad (8.81)$$

The exponent

$$\frac{2\nu-1}{6\nu-2} = 0 \quad \text{in } \theta \text{ - solvents } (\nu = 1/2), \quad (8.82)$$

Unentangled polymer dynamics

because the chain maintains a nearly ideal conformation at all concentrations and

$$\frac{2\nu - 1}{6\nu - 2} \cong 0.12 \quad \text{in good solvents } (\nu \cong 0.588). \quad (8.83)$$

The diffusion coefficient D in semidilute solutions decreases as a power law in concentration:

$$D \approx \frac{R^2}{\tau_{\text{chain}}} \approx \frac{kT}{\eta_s b} \frac{\phi^{-(1-\nu)/(3\nu-1)}}{N}. \quad (8.84)$$

The semidilute diffusion coefficient can be written in terms of the Zimm diffusion coefficient of the chain D_Z [Eq. (8.23) valid for diffusion in dilute solutions] and the overlap concentration $\phi^* \approx N^{-(3\nu-1)}$ [Eq. (5.19)]:

$$D \approx D_Z \left(\frac{\phi}{\phi^*} \right)^{-(1-\nu)/(3\nu-1)}. \quad (8.85)$$

The scaling exponent

$$\frac{1-\nu}{3\nu-1} = 1 \quad \text{in } \theta\text{-solvents } (\nu = 1/2), \quad (8.86)$$

and

$$\frac{1-\nu}{3\nu-1} \cong 0.54 \quad \text{in good solvents } (\nu \cong 0.588).$$

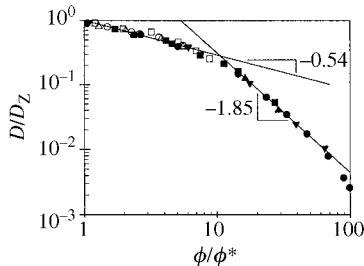


Fig. 8.9

Concentration dependence of diffusion coefficient in good solvent. Filled symbols are four molar masses of polystyrene in benzene spanning the range 78 000–750 000 g mol⁻¹, from L. Leger and J. L. Viovy, *Contemp. Phys.* **29**, 579 (1988). Open symbols are three molar masses of poly(ethylene oxide) in water spanning the range 73 000–660 000 g mol⁻¹, from W. Brown, *Polymer* **25**, 680 (1984). To facilitate comparison, ϕ^* was taken as the volume fraction at which $D = D_Z$ for each data set. The low concentration line is Eq. (8.85) and the high concentration line has the slope expected for entangled solutions in good solvent [Eq. (9.43)].

The concentration dependence of the diffusion coefficient is plotted in Fig. 8.9 in the scaling form suggested by Eq. (8.85) for polymer solutions in good solvents. The expected exponent is observed over a limited range of approximately one decade above the overlap concentration ϕ^* and a stronger concentration dependence is seen at higher concentrations, where entanglements become important.

In semidilute solutions, hydrodynamic interactions are not screened on length scales smaller than the correlation length ξ . Each mode involves coherent motion of N/p monomers. If N/p is smaller than the g monomers in a correlation blob, motion associated with that mode is described by the Zimm model. On larger length scales, hydrodynamic interactions are screened and modes with index $p < N/g$ are described by the Rouse model. The number of monomers in a correlation blob is given by Eq. (8.77). The crossover mode index for hydrodynamic interaction is

$$p_\xi = \frac{N}{g} \approx N\phi^{1/(3\nu-1)}. \quad (8.87)$$

There are three time scales important for the stress relaxation modulus in semidilute unentangled solutions. The shortest time scale is the relaxation time of a monomer [Eq. (8.20)]. The intermediate time scale is the

Zimm relaxation time corresponding to the correlation blob [Eq. (8.75)]. The longest time scale is the Rouse relaxation time of the chain of correlation blobs [Eq. (8.78)].

The stress relaxation modulus follows the Zimm dependence on time scales shorter than τ_ξ , corresponding to motion of chain sections smaller than the correlation length:

$$G(t) \approx \frac{kT}{b^3} \phi \left(\frac{t}{\tau_0} \right)^{-1/(3\nu)} \quad \text{for } \tau_0 < t < \tau_\xi. \quad (8.88)$$

At the crossover time $t = \tau_\xi$ [Eq. (8.75)] the stress relaxation modulus is of the order of the osmotic pressure:

$$G(\tau_\xi) \approx \frac{kT}{b^3} \phi^{3\nu/(3\nu-1)} \approx \frac{kT}{\xi^3} \approx \Pi. \quad (8.89)$$

At longer times, the stress relaxation modulus follows the Rouse dependence:

$$G(t) \approx \frac{kT}{b^3} \phi^{3\nu/(3\nu-1)} \left(\frac{t}{\tau_\xi} \right)^{-1/2} \quad \text{for } \tau_\xi < t < \tau_{\text{chain}}. \quad (8.90)$$

The value of the stress relaxation modulus at the relaxation time of the chain can be determined from Eq. (8.90):

$$G(\tau_{\text{chain}}) \approx \frac{kT}{b^3} \phi^{3\nu/(3\nu-1)} \left(\frac{\tau_{\text{chain}}}{\tau_\xi} \right)^{-1/2} \approx \frac{kT}{b^3} \phi^{3\nu/(3\nu-1)} \frac{g}{N} \approx \frac{kT}{b^3 N} \phi. \quad (8.91)$$

Equations (8.76) and (8.77) were used to simplify this expression for $G(\tau_{\text{chain}})$. The terminal modulus is of order kT per chain, as it must be for any unentangled flexible chain [see Eq. (8.32)]. The stress relaxation modulus at long times is approximated well by the product of the power law and an exponential cutoff:

$$G(t) \approx \frac{kT}{b^3 N} \phi \left(\frac{t}{\tau_{\text{chain}}} \right)^{-1/2} \exp(-t/\tau_{\text{chain}}) \quad \text{for } t > \tau_\xi. \quad (8.92)$$

The time dependence of the stress relaxation modulus in semidilute unentangled solution is sketched in Fig. 8.10. Experimental verification of Rouse dynamics for frequencies smaller than $1/\tau_\xi$ was shown in Fig. 8.5, for a semidilute unentangled polyelectrolyte solution.

The polymer contribution to viscosity in semidilute unentangled solutions is obtained by integrating the stress relaxation modulus over time [Eq. (7.117)].

$$\eta - \eta_s = \int_0^\infty G(t) dt \approx \frac{kT}{b^3} \frac{\phi}{N} \tau_{\text{chain}} \approx \eta_s N \phi^{1/(3\nu-1)}. \quad (8.93)$$

In Problem 8.21, the integration is shown to be controlled by the longest relaxation time τ_{chain} .

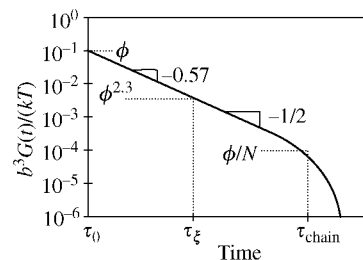


Fig. 8.10

Stress relaxation modulus of an unentangled semidilute solution of chains with $N = 10^3$ monomers at volume fraction $\phi = 0.1$ in an athermal solvent (logarithmic scales).

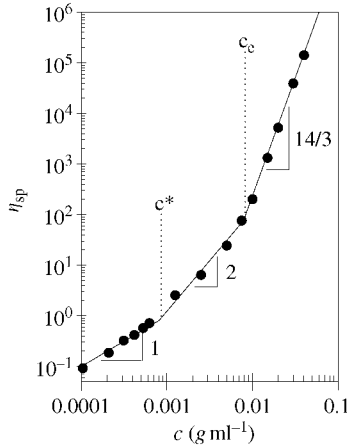


Fig. 8.11

Concentration dependence of specific viscosity for linear poly(ethylene oxide) with $M_w = 5 \times 10^6 \text{ g mol}^{-1}$ in water at 25.0°C . Data courtesy of S. Singh.

This result can alternatively be obtained from a de Gennes scaling argument. At the overlap concentration $\phi^* \approx N^{1-3\nu}$, the polymer contribution to viscosity is of the order of the solvent viscosity, and grows as a power law in concentration in semidilute solution:

$$\eta - \eta_s \approx \eta_s \left(\frac{\phi}{\phi^*} \right)^x. \quad (8.94)$$

The exponent x can be determined from the condition that the long-time modes are Rouse-like, and therefore the polymer contribution to solution viscosity should be linearly proportional to polymer molar mass:

$$\eta - \eta_s \approx \eta_s N^{(3\nu-1)x} \phi^x, \quad (8.95)$$

$$(3\nu - 1)x = 1 \Rightarrow x = \frac{1}{3\nu - 1}. \quad (8.96)$$

In θ -solvents ($\nu = 1/2$), the exponent $1/(3\nu - 1) = 2$, and the viscosity is predicted to grow as the square of polymer concentration in unentangled semidilute θ -solutions:

$$\eta_{\text{sp}} \approx N\phi^2 \approx \left(\frac{\phi}{\phi^*} \right)^2. \quad (8.97)$$

This concentration dependence is demonstrated in Fig. 8.11. In good solvents ($\nu \cong 0.588$), the exponent $1/(3\nu - 1) \cong 1.3$, and the viscosity is predicted to grow as a weaker power of concentration:

$$\eta_{\text{sp}} \approx N\phi^{1.3} \approx \left(\frac{\phi}{\phi^*} \right)^{1.3}. \quad (8.98)$$

8.6 Modes of a semiflexible chain

Polymer dynamics discussed in the previous sections of this chapter correspond to completely flexible chains and are related to modes on length scales larger than the Kuhn length. The relaxation mode structure on length scales shorter than the Kuhn length is significantly different. Many chains, in particular biopolymers, are locally quite stiff. A large part of the relaxation spectrum of such semiflexible chains corresponds to modes with wavelengths shorter than their Kuhn length. In this section, the mode spectrum of semiflexible chains without any intrinsic curvature or twist is described.

8.6.1 Bending energy and dynamics

Consider an elastic beam of length L , thickness L_y and width L_z with Young's modulus E . It is instructive to calculate the elastic energy of bending this beam by a small angle θ (see Fig. 8.12):

$$\theta \approx \sin\left(\frac{h_y}{L}\right) \approx \frac{h_y}{L}. \quad (8.99)$$

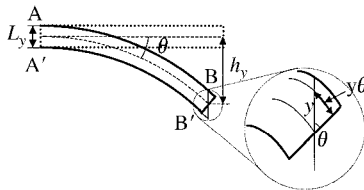


Fig. 8.12

Bending of a rod by angle θ . Insert: the elongation along a surface that is a distance y above the undeformed middle surface is $y\theta$ (and $y < 0$ below the middle surface, in compression).

The central part of the beam (dashed line in Fig. 8.12) is undeformed, the upper half of the beam (AB) is under tension, while the lower half (A'B') is under compression. The deformation along the plane of the bent beam a distance y away from the undeformed central surface is $\Delta L = y\theta$ (see insert in Fig. 8.12). The corresponding extensional strain is $\varepsilon(y) \equiv \Delta L/L = y\theta/L$. The elastic energy density is the work done by deformation per unit volume. Stress is force per unit cross-sectional area and strain is the deformation per unit length, so elastic energy density is proportional to the product of stress and strain $\sigma\varepsilon = E\varepsilon^2$, where E is Young's modulus. The elastic energy of a thin slice of the beam of thickness dy and cross-sectional area LL_z is $E(y\theta/L)^2 LL_z dy$. The total elastic energy of a bent beam is obtained by integrating the contribution from each slice over the thickness of the beam:

$$\begin{aligned} U_L(\theta) &\approx \int_{-L_y/2}^{L_y/2} E \left(\frac{y\theta}{L} \right)^2 LL_z dy \approx EL_z \frac{\theta^2}{L} \int_{-L_y/2}^{L_y/2} y^2 dy \\ &\approx EL_z \frac{\theta^2}{L} L_y^3. \end{aligned} \quad (8.100)$$

The Kuhn length b determines the crossover between stiff and flexible length scales. For rods or beams with length L of the order of the Kuhn length b , the angle of thermally induced fluctuations is of the order of unity $\theta \approx 1$:

$$U_b(1) \approx E \frac{L_y^3 L_z}{b} \approx kT. \quad (8.101)$$

This equation can be solved for the Kuhn length:

$$b \approx E \frac{L_y^3 L_z}{kT}. \quad (8.102)$$

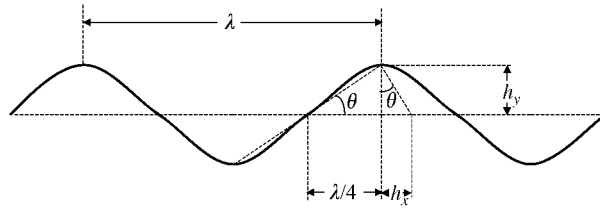
The bending energy of a bent beam [Eq. (8.100)] then can be rewritten in terms of the Kuhn length:

$$U_L(\theta) \approx kT \frac{b}{L} \theta^2 \approx kT \frac{b}{L} \left(\frac{h_y}{L} \right)^2. \quad (8.103)$$

The last relation was obtained using Eq. (8.99) for the deformation angle θ . By writing Eq. (8.103) in terms of the Kuhn length, it becomes much more general and applies to beams with cross-sections that are not rectangular (such as the bending of a cylindrical rod).

Since the beam or rod is a solid, it has natural modes of bending with wavelengths that allow the ends of the beam to be stationary. The first (longest wavelength) mode has wavelength $\lambda = 2L$, the second mode has $\lambda = L$, the third mode has $\lambda = 2L/3$, etc. The fourth mode (with $\lambda = L/2$) is illustrated in Fig. 8.13. Spontaneous thermally induced vibration modes of the beam will form at these wavelengths, and the amplitude of each mode

Unentangled polymer dynamics

**Fig. 8.13**

Schematic of the fourth vibration mode (with wavelength $\lambda = L/2$) of a rigid rod of length L . The transverse oscillation with amplitude h_y , reduces the projected rod length along the x-axis. The amount that the rod length is reduced, per wavelength λ , oscillates with longitudinal amplitude h_x .

is determined by setting the bending energy from Eq. (8.103) at length scale λ equal to the thermal energy kT :

$$U_\lambda \approx kTb \frac{h_y^2}{\lambda^3} \approx kT. \quad (8.104)$$

This equation can be solved for the mean-square amplitude of these modes in the transverse direction:

$$h_y^2 \approx \frac{\lambda^3}{b}. \quad (8.105)$$

To understand the dynamics of the bending fluctuations associated with these natural modes, a force balance per unit length is required. The force per unit length associated with the bending mode of wavelength λ is calculated by differentiating the energy U_λ and it is resisted by the frictional dissipation:

$$\frac{1}{\lambda} \frac{dU_\lambda}{dh_y} \approx kTb \frac{h_y}{\lambda^4} \approx -\frac{\zeta}{b} \frac{dh_y}{dt}. \quad (8.106)$$

To understand the frictional dissipation term, recall that the friction coefficient ζ of a Kuhn segment of length b is the ratio of force and velocity in a liquid. Hence, ζ/b is the ratio of force per unit length and the velocity dh_y/dt . This equation can be solved by separation of variables and integration:

$$\int \frac{dh_y}{h_y} \approx -\frac{kTb^2}{\zeta\lambda^4} \int dt. \quad (8.107)$$

The solution is exponentially decaying in time $h_y \sim \exp(-t/\tau)$ with relaxation time τ proportional to the fourth power of the wavelength λ of the mode:

$$\tau \approx \frac{\zeta}{kTb^2} \lambda^4. \quad (8.108)$$

Alternatively, the wavelength of a bending mode is proportional to the 1/4 power of its relaxation time:

$$\lambda \approx \left(\frac{kTb^2}{\zeta} t \right)^{1/4} \approx b \left(\frac{kT}{\zeta b^2} t \right)^{1/4} \approx b \left(\frac{t}{\tau_0} \right)^{1/4}. \quad (8.109)$$